Effects of Base Sequence Context on Translesion Synthesis Past a Bulky (+)-*trans-anti*-B[*a*]P-N^2-dG Lesion Catalyzed by the Y-family Polymerase pol κ[†]

Xuanwei Huang,[‡] Alexander Kolbanovskiy,[‡] Xiaohua Wu,[§] Yanbin Zhang,[§] Zhigang Wang,[§] Ping Zhuang,[‡] Shantu Amin,[||] and Nicholas E. Geacintov*[,‡]

Department of Chemistry, New York University, 31 Washington Place, New York, New York 10003-5180, Graduate Center for Toxicology, University of Kentucky, Lexington, Kentucky 40536, and American Health Foundation, Valhalla, New York 10595

Received September 27, 2002; Revised Manuscript Received January 3, 2003

ABSTRACT: The effects of bases flanking single bulky lesions derived from the binding of a benzo[*a*]pyrene 7,8-diol 9,10-epoxide derivative ((+)-7*R*,8*S*,9*S*,10*R* stereoisomer) to N^2-guanine (G*) on translesion bypass catalyzed by the Y-family polymerase pol κ (hDinB1) were examined in vitro. The lesions were positioned near the middle of six different 43-mer 5′-...XG*Y... sequences (X, Y = C, T, or G, with all other bases remaining fixed). The complementary dCTP is preferentially inserted opposite G* in all of the sequences; however, the proportions of other dNTPs inserted varies as a function of X and Y. The dCTP insertion efficiencies, $f_{ins} = (V_{max}/K_m)_{ins}$, are smaller in the XG*Y than in XGY sequences by factors of ∼50−90 (GG*T and GG*C) or 5000−25000 (TG*G and CG*G). Remarkably, in XG*Y sequences, f_{ins} varies by as much as 3 orders of magnitude, being smallest with G flanking the lesions on the 3′-side and highest with G flanking the adducts on the 5′-side. One-step primer extension efficiencies just beyond the lesions (f_{ext}) are generally smaller than f_{ins} and also depend on base sequence. However, reasonably efficient translesion bypass of the (+)-*trans*-[BP]-N^2-dG adducts is observed in all sequences in running-start experiments with full, or nearly full, primer extension being observed under conditions of [dNTP] > K_m. The key features here are the relatively robust values of the kinetic parameters V_{max} that are either diminished to a moderate extent or even enhanced in the presence of the (+)-*trans*-[BP]-N^2-dG adducts. In contrast to the small effects of the lesions on V_{max}, the apparent K_m values are orders of magnitude greater in XG*Y than in the unmodified XGY sequences. Thus the bypass of (+)-*trans*-[BP]-N^2-dG adducts under conditions when [dNTP] < K_m is quite inefficient. These considerations may be of importance in vivo where [dNTP] ≤ K_m, and the translesion bypass of the (+)-*trans*-[BP]-N^2-dG by pol κ may be significantly less efficient than in vitro at higher dNTP concentrations. The base sequence-dependent features of translesion bypass are discussed in terms of the possible conformations of the adducts and the known structural features of bypass polymerases.

The recently discovered polymerase pol κ (*1*−*3*) is encoded by the human *DinB1* gene and belongs to the Y-family of DNA polymerases (*4*). The Y-family polymerases are characterized by their low-fidelity replication of normal DNA (*2*, *5*, *6*) and by their ability to bypass a variety of DNA lesions in vitro. Human pol κ is a distributive enzyme that lacks a proofreading 3′-5′ exonucleolytic activity (*6*, *7*). Purified human pol κ bypasses 8-*oxo*-7,8-dihydrodeoxyguanine (*8*), 1,N^6-ethenodeoxyadenosine (*9*), and abasic sites (*1*, *8*); however, the bypass of abasic sites depends on the sequence context 5′- to the lesion (*1*, *3*, *5*, *8*). Pol κ is unable to bypass either cisplatin adducts (*1*, *3*) or thymine dimers (*1*, *8*). On the other hand, this polymerase can bypass bulky lesions such as those derived from the reactions of *N*-acetyl 2-aminofluorene with C^8-dG (*1*, *3*, *8*, *10*). Another bulky lesion that can be bypassed by pol κ is the adduct derived from the binding of *anti*-BPDE[1] ((+)-7,8-dihydroxy-*anti*-9,10-epoxy-7,8,9,10-tetrahydrobenzo[*a*]pyrene), a potent mutagen derived from the metabolic activation of the ubiquitous environmental pollutant benzo[*a*]pyrene, to DNA (*8*, *11*−*13*). The diol epoxide *anti*-BPDE reacts preferentially with the exocyclic amino group of guanine in DNA to form covalent [BP]-N^2-dG adducts (*14*). It is well-established that such adducts (Figure 1), site-specifically incorporated into oligonucleotide template strands, are strong blocks to DNA synthesis catalyzed by high fidelity replicative polymerases in vitro (*15*−*20*). Site-specific mutagenesis experiments in cellular systems indicate that the mutagenic properties of

[†] This work was supported by NIH/NCI Grants CA 20851 and CA 76660 (N.E.G.), NIH/NCI CA 92768 (Z.W.), and CB-77022−75 (S.A.).

* Corresponding author. Tel: (212) 998-8407. Fax: (212) 998-8421. E-mail: ng1@nyu.edu.

[‡] New York University.

[§] University of Kentucky.

[||] American Health Foundation.

[1] Abbreviations: BP, benzo[*a*]pyrene; (+)-*anti*-BPDE, (+)-7*R*,8*S*-dihydroxy-9*S*,10*R*-epoxy-7,8,9,10-tetrahydrobenzo[*a*]pyrene; (+)-*trans-anti*-[BP]-N^2-dG adducts, covalent products derived from the binding of (+)-*anti*-BPDE, at its C10 position, to the N^2-2′-deoxyguanosine residues in DNA by trans addition; EDTA, ethylenediaminetetraacetate; dNTP, 2′-deoxynucleoside 5′-triphosphate; f_{ins}, efficiency of dNTP insertion opposite the (+)-*trans-anti*-BP-N^2-dG lesion; f_{ext}, efficiency of single dNTP extension one base beyond the (+)-*trans-anti*-BP-N^2-dG lesion.

10.1021/bi026912q CCC: $25.00 © 2003 American Chemical Society
Published on Web 02/06/2003

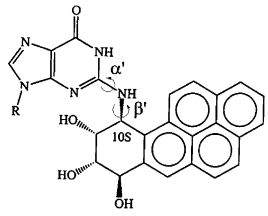

10S (+)-*trans-anti*-[BP]-N^2-dG

FIGURE 1: Structure of the (+)-*trans-anti*-[BP]-N^2-dG adduct (G*).

[BP]-N^2-dG lesions are functions of the cell system in which the mutations are expressed, as well as the adduct stereochemistry, and the base sequence context (*17*, *21*−*29*). The most frequently observed mutations are G → T transversions both in vitro and in vivo (*17*, *20*−*23*, *26*, *28*, *29*), but G → A and G → C base substitution are also observed (*25*−*27*).

Translesion synthesis past [BP]-N^2-dG adducts catalyzed by pol κ (*8*, *11*, *13*, *30*) and a truncated analogue of this polymerase, pol κ ΔC (*12*), have been observed. Unlike some of the replicative polymerases, pol κ not only bypasses the [BP]-N^2-dG lesions with surprising efficiency but also incorporates predominantly the correct dCTP opposite the adduct. Ogi et al. have shown that pol κ-deficient, mutant mouse embryonic stem (ES) cells are highly sensitive to both lethality and mutagenesis induced by B[*a*]P and thus concluded that pol κ plays an important role in suppressing mutations associated with DNA lesions derived from B[*a*]P in wild-type cells (*31*).

The translesion bypass activity of pol κ in vitro has been studied only in the case of *trans*-[BP]-N^2-dG adducts in a 5′-...CG*C... sequence context (*8*, *12*). Effects of flanking bases on the efficiencies and fidelities of replication have been noted in site-specific mutagenesis experiments with (+)-*trans*-[BP]-N^2-dG adducts in vitro (*17*, *19*, *20*, *32*−*34*) and in vivo (*17*, *22*, *23*, *25*−*27*, *29*). However, with one exception (*20*), these studies were not explicitly designed to uniquely probe the effects of different bases flanking the [BP]-N^2-dG adducts while all other bases in the sequence remained unchanged. Overall, the effects of base sequence context on mutagenesis associated with such bulky lesions are presently not well-understood. Loechler and co-workers proposed that different [BP]-N^2-dG adduct conformations can give rise to different base substitution mutations and that these conformations depend strongly on the bases flanking the adducts (*35*−*40*). A limited number of observations indicate that the conformational characteristics of [BP]-N^2-dG adducts are indeed dependent on the bases flanking the lesions (*41*−*43*) and thus could affect the efficiencies and specificities of translesion bypass (*35*, *37*).

In this work, we systematically investigated the effects of substituting the bases C, T, or G one at a time, flanking the (+)-*trans*-[BP]-N^2-dG adducts, on translesion bypass employing 43-mer template strands in which all other bases remained unchanged. Some of the same sequences were employed previously in studies of translesion bypass employing the exonuclease-free Klenow fragment, KF-, a classical replicative polymerase fragment from *Escherichia coli* pol I. The extent of lesion bypass was generally limited except in sequence contexts that allowed for the formation of slipped frameshift intermediates that yielded primer extension products with various deletions (*20*). Here, pol κ was selected as the polymerase because it is known to readily bypass [BP]-N^2-dG adducts (*8*, *11*, *13*, *30*) thus allowing for studies of base sequence effects on translesion synthesis. It is shown that the insertion of dCTP opposite the lesion is dominant in all sequence contexts studied, although in different proportions relative to the efficiencies of insertion of the other three 2′-deoxyribonucleotide triphosphates (dNTP). The kinetic parameters of insertion opposite the lesion and extension beyond the lesion are remarkably dependent on base sequence context. We show that the simple exchange of one flanking base with another can alter the efficiencies of single base insertion opposite the lesion by as much as 2−3 orders of magnitude. Large enhancements in efficiencies of translesion bypass are observed with G adjacent to the adduct on the 5′-side, while substantially lower efficiencies are observed when the G is positioned on the 3′-side. Possible mechanisms of these and other base sequence effects are discussed.

Scheme 1: 43-mer Template and Primer Strands Used in the Human pol κ-catalyzed Primer Extension Experiments and Translesion Synthesis Past [BP]-N^2-dG Adducts (G*) in XG*Y Sequences[a]

ZTGTGCGATAGACCGGTCTAGGCG-5′(^{32}P)
5′-GACTACGTACTGTCACAXG*YACACGCTATCTGGCCAGATCCGC-3′
40 30 25 20 10 1

[a] The length of the primer strand corresponds to the standing-start, single dCTP insertion experiments (Z: base complementary to Y in the template strands).

MATERIALS AND METHODS

Chemicals and Enzymes. All chemicals were analytical grade. [γ-^{32}P] ATP (3000 ci/mmol) was purchased from Perkin-Elmer Life Sciences, Inc. (Boston, MA). T7 DNA polymerase (Sequenase version 2.0) was purchased from Amersham Biosciences, Inc. (Piscataway, NJ). The dNTPs were purchased from New England Biolabs, Inc. (Beverly, MA). Pol κ was prepared as described (*6*, *8*). The concentration of the stock solution of pol κ was 15 ng/μL and that of T7 polymerase was 13 units/μL.

Oligonucleotides. 11-mer oligonucleotides with a central triple base motif CACAXGYACAC (X, Y = C, T, or G) were synthesized by standard phosphoramidite methods on a Biosearch Cyclone automated DNA synthesizer (Milligen-Biosearch Corp., San Rafael, CA) and were purified and desalted by standard HPLC protocols (*44*). The synthesis, purification, and characterization of the site-specifically modified 11-mer oligonucleotides CACAXG*YACAC with single (+)-*trans*-[BP]-N^2-dG lesions have been fully described elsewhere (*45*, *46*). The compositions of the modified and unmodified 11-mer sequences were verified by mass spectrometry using a Bruker Daltonics OmniFlex MALDI TOF MS system. The site-specifically modified oligodeoxynucleotides were ligated to a 13-mer and a 19-mer to form 43-mer template strands (Scheme 1) as previously described (*20*). The ligated 43-mer template strands were purified on a 20% polyacrylamide gel with 7 M urea, visualized by ethidium bromide staining, and eluted, and the ethidium bromide was extracted from the aqueous fraction with butanol. The ligated oligonucleotide was further purified and desalted by three successive ethanol precipitations. The quality of the sample was rechecked by gel electrophoresis (the BP-modified oligonucleotide migrates somewhat slower than the unmodified one), and fluorescence and UV absorp-

tion spectroscopy were employed to further verify that the BP residue was intact (*47*).

Running-Start DNA Replication as a Function of Time. The 43-mer unmodified or modified templates with single (+)-*trans*-[BP]-N^2-dG lesions were annealed with a γ^{32}P-ATP labeled 22-mer primer at a 1.5:1 ratio. The primer extension reactions were performed in a 10 μL reaction solution containing 25 mM KH_2PO_4 (pH 7.0), 5 mM $MgCl_2$, 5 mM dithiothreitol, 100 μg/mL bovine serum albumin, 10% glycerol, 100 μM of dNTPs, 2.5 nM primer/template complex, and 3.75 ng of pol κ (~38 fmol or 3.8 nM). This amount of polymerase was selected because it afforded a comparison of primer extension activity using both BPDE-modified and unmodified templates under identical solution conditions. The reaction was allowed to proceed at 30 °C for selected times before being terminated with 7 μL of stop solution (20 mM EDTA, 95% formamide, 0.05% bromophenol blue, and 0.05% xylene cyanol). This particular temperature was selected to monitor the activity of the polymerase under conditions used earlier by the Z. Wang group (*8*). Because purified pol κ is unstable under ambient conditions, samples of the polymerase were divided into small aliquots and stored at −80 °C. Each aliquot was used only once. Thus, the polymerase samples exhibited the same activities in different experiments since all samples were thawed only once before the experiments were performed.

The reaction mixtures were then heated to 90 °C for 5 min, followed by chilling in ice water, and subjected to 20% denaturing polyacrylamide gel electrophoresis, followed by quantitative analysis using a Storm 840 phosphorimager and the Storm ImageQuant software (Amersham).

Standing-Start dNTP Insertion Fidelity Assay. The 43-mer BPDE-modified templates were annealed with a γ^{32}P-ATP labeled 24-mer primer at a template/primer ratio of 1.5:1. The terminal 3′-base of this primer extended up to the template base flanking the adduct on the upstream 3′-side. The mutational specificity assay using human pol κ was carried out under the same reaction conditions as the running-start replication experiment, except that the dNTP concentration was 200 μM.

Determination of V_{max} and K_m Values. The steady-state kinetics of single dNTP insertion opposite the (+)-*trans*-[BP]-N^2-dG adduct, or extension one base beyond the lesion by human pol κ, were determined using the basic methodology described previously (*48*) with slight modifications (*20*). Briefly, the assays were performed in a 10 μL reaction solution containing 25 fmol (2.5 nM) of a primed DNA template, 3.75 ng of purified pol κ (~3.8 nM), and variable concentrations of dCTP for insertion or, in the case of extension, of a single dNTP (complementary to X in the 43mer ...XG*Y...sequence). These concentrations were selected to compare the efficiencies, under identical conditions, of primer extension using modified and unmodified templates. After incubating at 30 °C for selected times under standard DNA polymerase assay conditions, the reactions were terminated, and the reaction products were separated by electrophoresis on a 20% denaturing polyacrylamide gel. The percentage of primers extended was estimated from the phosphorimager densitometry scans and were repeated three times. The observed rate of reaction (V) was then plotted as a function of dNTP concentration, and the parameters V_{max} and K_m were estimated from the best nonlinear regression fit of the Michaelis−Menten equation

$$V = (V_{max} \times [\text{dNTP}])/(K_m + [\text{dNTP}]) \qquad (1)$$

using SigmaPlot software. The insertion and extension efficiencies were calculated from the expression f_{ins} (or f_{ext}) = (V_{max}/K_m) and are the averages of three independent experiments. Because it is difficult to prepare pol κ with an activity of 100%, the exact specific activity of the enzyme in our preparations cannot be specified. Therefore, the calculated values of the specific rate parameter $k_{cat} = V_{max}/[E_o]$, where E_o is the total enzyme concentration, are relative or apparent values.

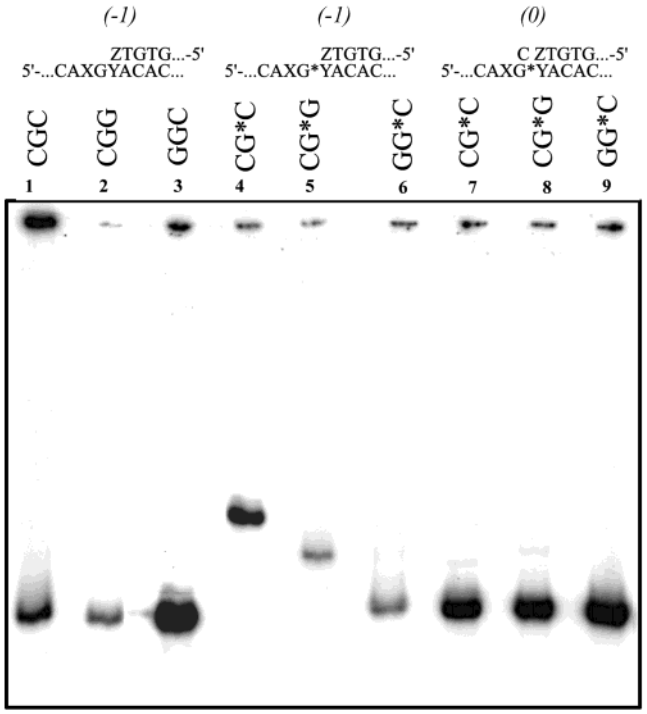

FIGURE 2: Mobilities of primer/template complexes in native 12% polyacrylamide gels.

RESULTS

Gel Electrophoretic Properties of Primer/Template Complexes. During the course of checking for proper primer/template complex formation by native polyacrylamide gel electrophoresis techniques, it was noted that the primer/template complexes exhibited unusual base sequence-dependent electrophoretic mobilities (Figure 2). With primer strands extending up to the 3′-base flanking lesion Y, termed (−1) complexes (an example is shown in Scheme 1), the electrophoretic mobilities depend remarkably on the base sequence context. The mobilities are unusually slow in the case of the CG*C and TG*T templates, intermediate in the case of the CG*G and TG*G templates, and fastest in the case of the GG*C and GG*T 43-mer templates in the (−1) complexes (lanes 4−6, respectively). Results for the TG*T, TG*G, and GG*T (−1) primer/template complexes are depicted in Figure S7, Supporting Information. These effects are not observed in the case of the analogous unmodified primer/template (−1) complexes (lanes 1−3). In the case of the (0) complexes (the 3′-base at the primer terminus is

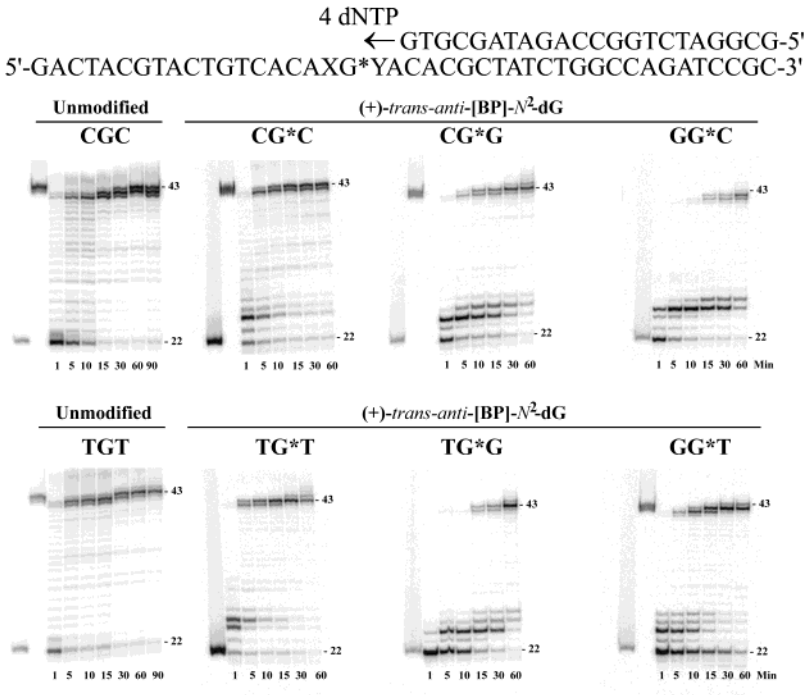

FIGURE 3: Running-start primer extension reaction experiments catalyzed by human pol κ on (+)-*trans*-[BP]-N^2-dG modified DNA templates XG*Y as a function of reaction time. The first two lanes on the left contain 22-mer primer and 43-mer marker sequences. Some typical experiments for the unmodified CGC and TGT sequences are also shown for comparison. The experimental conditions were identical in all experiments (see text).

positioned opposite G*), the electrophoretic mobilities of all complexes with modified guanines (lanes 7−9) closely resemble those of the unmodified (0) complexes (data not shown) and those of the unmodified (−1) complexes (lanes 1−3). These results indicate that the local structures at the single strand−double strand junctions in (−1) complexes are different in each of the complexes and that these give rise to various extents of local bending or loci of flexibility. It is evident that the structures of the primer/template junctions with (+)-*trans*-[BP]-N^2-dG adducts at the single strand−double strand junctions are remarkably dependent on the bases flanking the lesions in (−1) but not in the (0) complexes. The mobilities are determined by the positions of the flanking G and T or C bases and are independent of the nature of the pyrimidines. The striking sequence dependence of these effects (Figure 2) is a novel observation, although anomalously slow electrophoretic mobilities with (+)-*trans*-[BP]-N^2-dG lesions at the junctions have been observed with other primer/template complexes but only in ...CG*C... sequence contexts (*49*, *50*).

Running-Start Primer Extension on Unmodified and BPDE-Modified Templates. A survey of primer extension patterns catalyzed by pol κ is shown in Figure 3. The template/primer and enzyme concentrations were selected to allow direct comparisons of translesion bypass between modified and unmodified DNA templates. The primer 3′-terminus extends up to template position 22 counted from the 3′-end, three nucleotides upstream from the lesion at position 25 (Scheme 1). In the case of the unmodified sequences, as illustrated here with the CGC and TGT sequences (Figure 3), pol κ readily extends the primer strand almost to the end of the template after a 15 min incubation time under our experimental conditions. Primer extension stalls one or two nucleotides prior to the 5′-end of the unmodified template as reported earlier (*2*, *8*). However, upon extending the reaction time to 30 or 60 min, full 43-mer extension products are formed as observed by Ohashi et al. at higher enzyme concentrations (*1*).

In the case of the BPDE-modified templates, translesion bypass is observed in all cases although the polymerase pauses in the vicinity of the adducts in a sequence-dependent manner (Figure 3). At the dNTP concentrations used in these running-start experiments (100 μM of each dNTP), the lesions in the CG*C and TG*T sequence contexts are easily bypassed, although the polymerase pauses briefly at template position 24, just before the adduct. In the case of the TG*T sequence, it also stalls briefly at position 25 with the 3′-terminal base of the primer opposite the lesion. In all other sequences, stalling is more pronounced at positions 24, except in the GG*C sequence that exhibits a prominent stall site when the primer strand extends to position 25. Given sufficient reaction time, full-length extension products (43-mers) are observed in all modified sequences, except in the case of the GG*C and GG*T sequences. In the latter two sequences, 42-mers are dominant.

Sequence Dependence of Fidelity of Nucleotide Insertion Opposite the Lesion. Using T7 (Sequenase version 2.0) as a representative A-family polymerase, adenine is preferentially incorporated opposite the (+)-*trans*-[BP]-N^2-dG adducts in all six sequence contexts studied here (Supporting Information, Figure S1), as observed in other experiments with purified polymerases (*16*−*20*). These results indicate that the sequences selected for study here are not unusual with respect to their response to a classical, replicative A-family polymerase. The results of typical single dNTP insertion experiments opposite the (+)-*trans*-[BP]-N^2-dG adduct flanked by different bases catalyzed by pol κ are depicted in Figure 4. While dCTP insertion exceeds the incorporation of any

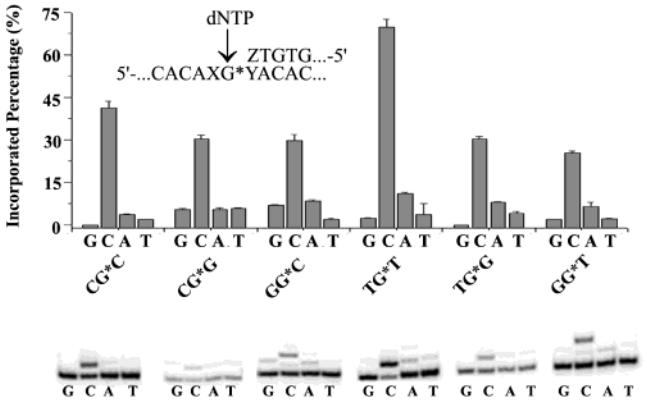

FIGURE 4: Single dNTP incorporation selectivity opposite the adduct (G*) catalyzed by human pol κ as a function of different template bases flanking the (+)-*trans*-[BP]-N^2-dG adducts in the 43-mer XG*Y template sequences.

of the other three dNTPs in all of the sequences studied (Figure 4), as well as in another CG*C sequence context investigated (*12*), the relative proportions of different dNTPs incorporated do depend on the bases flanking G*. In contrast to pol κ, dCTP is the least efficiently inserted dNTP opposite the lesions in the case of T7 polymerase (Figure S1, Supporting Information); primer extension beyond the lesion is almost completely blocked (*51*) as observed by others (*32*).

Kinetics of Single Nucleotide Incorporation Opposite G Catalyzed by pol κ.* The kinetic parameters V_{max} and K_m were compared for all six of the BPDE-modified and unmodified sequences for dCTP insertion opposite the lesion and extension by one dNTP opposite the base flanking G* on the 5′-side. Examples of typical single-dNTP insertion experiments are depicted in Figure 5. These standing-start experiments were designed to ensure that less than 20% of the initial primer strands were extended (*48*, *52*). The rate of primer extension was plotted as a function of the dNTP concentrations (Figure 5), and the parameters $(V_{max})_{ins}$ and K_m were extracted from the best fits to the data points of the Michaelis−Menten equation (eq 1). The results are provided in numerical form in Tables 1 and 2 and in the form of bar graphs in Figures 6−8. The calculated values of k_{cat} are also shown in the tables.

The values of the insertion efficiencies $f_{ins} = (V_{max}/K_m)_{ins}$ opposite the BPDE-modified guanine residue G* = (+)-*trans*-[BP]-N^2-dG are depicted in Figure 6, upper panel. The data are presented in terms of a semilogarithmic scale because of the surprisingly large variations in the f_{ins} values. The values of this parameter can be roughly grouped into three categories: (1) the largest values (sequences with 5′-flanking Gs), (2) intermediate values (pyrimidines on both sides), and (3) smallest values (sequences with 3′-flanking Gs). Remarkable variations in the f_{ins} values over a range of nearly 3 orders of magnitude are observed when the positions of two bases are interchanged between the 5′- and the 3′-side of the lesion G* (compare, for example, the f_{ins} values for GG*C and CG*G). Smaller but still substantial effects are observed when only one base is interchanged. For example, when a 3′-flanking C is replaced by a G (compare CG*C vs CG*G), the f_{ins} value decreases by a factor of nearly 200. In summary, a guanine flanking the adduct G* on the 5′-side instead of a C or a T significantly increases dCTP incorporation opposite the lesion, while a guanine replacing a C or T on the 3′-side diminishes f_{ins}.

To further understand the effects of the flanking bases, it is of interest to separately examine the values of $(V_{max})_{ins}$ and $(K_m)_{ins}$. The individual values of V_{max} are depicted in the upper panels of Figures 7 and 8, respectively. The major sequence-dependent effects on dNTP insertion opposite the (+)-*trans*-[BP]-N^2-dG adducts are illustrated by the dNTP concentration-dependence plots for the CG*C, CG*G, and GG*C sequences shown in Figure 5. Analogous sequence effects are observed in the case of the TG*T, TG*G, and GG*T sequences (Table 1 and Figure S6 in Supporting Information). The major sequence-dependent effects can be summarized as follows:

(1) The dCTP concentrations needed to approach saturating values of the insertion rates ($V_{ins} = (V_{max})_{ins}$) are more than 20 times greater in the case of the CG*G and TG*G sequences than in the other four sequences. With G on the 3′-side of the lesion, the K_m values are unfavorable and 1−2 orders of magnitude larger than in the GG*C, GG*T, CG*C, and TG*T sequences (Figure 8 and Table 1).

(2) The rates of dCTP insertion opposite the lesion and the $(V_{max})_{ins}$ values are highest when the 5′-flanking base is G (Figures 5 and 7, respectively), regardless of the 3′-flanking base (C or T).

(3) Only minor differences are observed in $(V_{max})_{ins}$ when a single T or C is interchanged in the TG*T and CG*C, and GG*T and GG*C sequences. However, when the 5′-flanking T in TG*G is replaced by a C, the $(V_{max})_{ins}$ is a factor of ∼10 smaller in CG*G. Relatively small variations in K_m are observed when one pyrimidine is replaced by the other in all sequences (Figure 8).

Extension Kinetics by a Single Nucleotide Beyond the Lesion. For each of the six sequences, the dNTP used was complementary to the flanking template base X in the XG*Y sequences (Figures 6−8, lower panels). The variations in f_{ext} as a function of the flanking bases are much less pronounced than in the case of f_{ins}. The largest decrease in the f_{ext} values, by a factor of about 10, is observed in the case of the TG*T and TG*G sequences when the 3′-flanking T in TG*T is replaced by a 3′-flanking G. With a G flanking the adducts on the 5′-side, the f_{ext} values are 20−50 times smaller than the f_{ins} values (Figure 6, Table 1). However, in the other sequences, except in CG*G, the insertion and extension efficiencies are similar in magnitude. In the CG*G sequence, f_{ext} is ∼10 times larger than f_{ins}.

Comparisons of V_{max} and K_m for BPDE-Modified and Unmodified Sequences. In the case of the unmodified sequences, XGY, the Michaelis−Menten parameters $(V_{max})_{ins}$ and $(K_m)_{ins}$ for catalysis by pol κ at position 25 of the template strand are fairly independent of the flanking bases X and Y, with the exception of the unmodified TGT sequence, which exhibits a 3-fold greater value of f_{ins} than the other five sequences (Figures S2−4, upper panels, and Table 2). Relatively minor variations are observed in the values of $f_{ext} = (V_{max}/K_m)_{ext}$ as a function of base sequence context (Table 2 and Figure S2 in Supporting Information). An unusually high value is observed only in the case of the TGT sequence.

These results indicate that the sequence effects reported here are attributable to the lesions rather than to intrinsic sequence contexts associated with the unmodified sequences. Comparisons of the $(V_{max})_{ins}$ values for the unmodified and

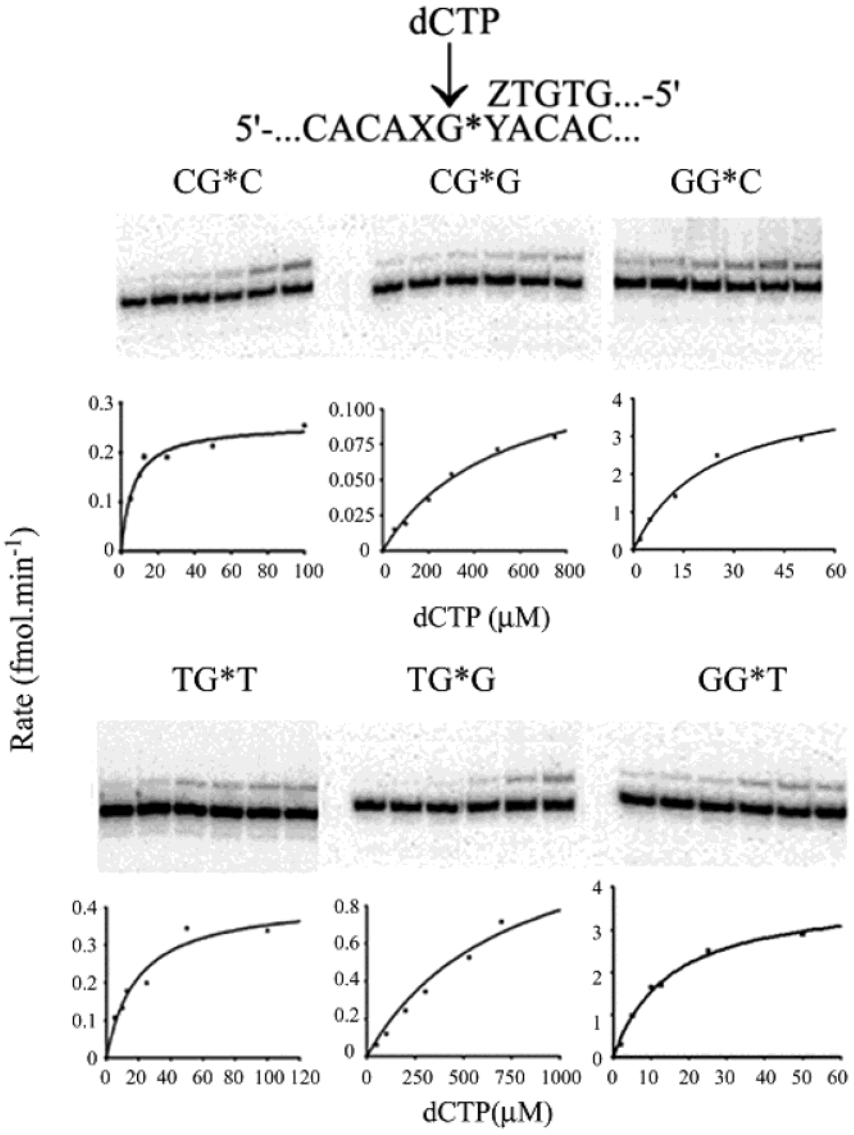

FIGURE 5: Dependence of rate of reaction on dCTP concentration catalyzed by pol κ for the XG*Y sequences for insertion of the dCTP opposite G* under identical reaction conditions.

BPDE-modified sequences measured under identical experimental conditions (Tables 1 and 2) reveal that the differences are small relative to the observed differences in the $(K_m)_{ins}$ values. The differences in $(V_{max})_{ext}$ between all six modified and unmodified sequences are all within factors of ~1.5−4. However, the $(K_m)_{ext}$ values are 2−5 orders of magnitude larger in the modified than in the unmodified sequences. The presence of a flanking T on either side of G*, especially on the 5′-side, is correlated with particularly high $(K_m)_{ext}$ values.

DISCUSSION

Impact of (+)-trans-[BP]-N^2-dG Adducts on Translesion Bypass. The efficiencies of translesion bypass are significantly reduced by the presence of the (+)-*trans*-[BP]-N^2-dG adducts. Depending on the sequence context, the insertion efficiency of dCTP opposite the lesion, f_{ins}, is 2−4 orders of magnitude smaller in the case of the BPDE-modified than in the case of the unmodified primer/template complexes with the same sequence contexts. The lesions also have an adverse impact on the extension efficiencies since f_{ext} is 2−5 orders of magnitude smaller in the modified than in unmodified templates (Tables 1 and 2). The largest base sequence effects are observed when either pyrimidine flanking the lesion is replaced by guanine. In the following, we consider the efficiencies of translesion bypass in terms of DNA adduct conformations and structures of polymerases and discuss possible interpretations of the observed effects of the bases flanking the lesions. Finally, we discuss the bypass characteristics of pol κ in terms of the observed blocking effects of the [BP]-N^2-dG adducts.

Structural Considerations. Recent determinations of the crystal structures of several bypass polymerases with and without substrates (*53*−*55*) are beginning to provide insights into possible mechanisms of translesion bypass (*56*). In particular, the crystal structure of a ternary complex of a primer/template with a dNTP at the active site of the polymerase Dpo4, a DinB homologue from the archeal aerobic thermophile *Sulfolobus solfataricus* P2, provides useful insights into the structural characteristics of this member of the Y-family polymerases (*55*).

The catalytic core subdomain of Dpo4 resembles the structure of classical A-family polymerases with right-handed palm, thumb, and finger motifs. However, in A-family polymerases, the two bulky O and O1 helices in the finger

Table 1: Efficiencies of Base Incorporation Opposite the (+)-*trans-anti-N*^{2}-dG Lesions and Base Extension beyond this Lesion in the Different XG*Y Sequences Catalyzed by Human pol κ

insertion/ extension	adduct sequence XG*Y	base pairing	V_{max} (fmol/min)	K_m (μM)	V_{max}/K_m (fmol min^{-1} μM^{-1}) $\times 10^3$	k_{cat}[a] (min^{-1}) $\times 10^3$
insertion	CG*C	G*:dCTP	0.250 ± 0.011	5.07 ± 1.78	49.7 ± 19.5	6.59
	CG*G	G*:dCTP	0.140 ± 0.015	510 ± 154	0.270 ± 0.110	3.68
	GG*C	G*:dCTP	4.38 ± 0.52	22.8 ± 5.9	192 ± 73	115
	TG*T	G*:dCTP	0.420 ± 0.050	19.2 ± 6.0	21.9 ± 9.4	11.1
	TG*G	G*:dCTP	1.35 ± 0.30	734 ± 294	1.84 ± 1.14	35.5
	GG*T	G*:dCTP	3.85 ± 0.24	15.0 ± 2.3	258 ± 55	101
extension	CG*C	C:dGTP	0.920 ± 0.050	113 ± 10	8.13 ± 1.14	24.2
	CG*G	C:dGTP	0.530 ± 0.170	150 ± 72	3.55 ± 2.85	13.9
	GG*C	G:dCTP	0.220 ± 0.010	22.4 ± 3.0	9.66 ± 1.92	5.79
	TG*T	T:dATP	1.34 ± 0.29	101 ± 36	13.2 ± 7.5	35.3
	TG*G	T:dATP	0.710 ± 0.040	623 ± 73	1.14 ± 0.20	18.7
	GG*T	G:dCTP	0.970 ± 0.020	207 ± 25	4.68 ± 0.66	25.5

[a] Apparent k_{cat} values are calculated from $V_{max}/[E_0]$. $[E_0]$ is the total enzyme concentration.

Table 2: Efficiencies of Base Incorporation Opposite G and Base Extension beyond This Base in the Different Unmodified XGY Sequences Catalyzed by Human Pol κ

insertion/ extension	adduct sequence XGY	base pairing	V_{max} (fmol/min)	K_m (μM) $\times 10^3$	V_{max}/K_m (fmol min^{-1} μM^{-1}}	k_{cat}[a] (min^{-1}) $\times 10^3$
insertion	CGC	G:dCTP	1.31 ± 0.11	74.4 ± 13.7	17.5 ± 4.7	34.5
	CGG	G:dCTP	2.27 ± 0.83	332 ± 174	6.80 ± 0.61	59.7
	GGC	G:dCTP	1.65 ± 0.14	98.9 ± 17.1	16.7 ± 4.3	43.4
	TGT	G:dCTP	1.31 ± 0.07	26.8 ± 4.3	48.7 ± 10.5	34.5
	TGG	G:dCTP	2.24 ± 0.75	247 ± 130	9.10 ± 7.80	58.9
	GGT	G:dCTP	1.69 ± 0.06	126 ± 8	13.5 ± 1.3	44.5
extension	CGC	C:dGTP	1.57 ± 0.34	128 ± 35	12.3 ± 6.1	41.3
	CGG	C:dGTP	2.13 ± 0.30	90.9 ± 17.6	23.5 ± 7.9	56.1
	GGC	G:dCTP	1.16 ± 0.23	131 ± 48	8.82 ± 4.90	30.5
	TGT	T:dATP	2.26 ± 0.04	0.69 ± 0.30	3260 ± 1240	59.5
	TGG	T:dATP	0.172 ± 0.003	5.78 ± 0.51	29.8 ± 3.2	4.53
	GGT	G:dCTP	0.388 ± 0.026	9.83 ± 1.90	39.4 ± 0.3	10.2

[a] Apparent k_{cat} values are calculated from $V_{max}/[E_0]$. $[E_0]$ is the total enzyme concentration.

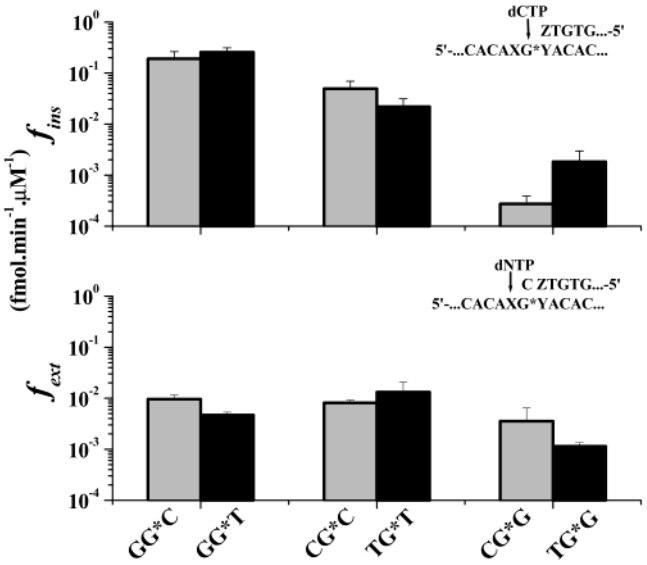

FIGURE 6: Dependence on the bases flanking the lesion G* of the steady-state dCTP insertion efficiency, $f_{ins} = (V_{max}/K_m)_{ins}$, opposite the modified guanine lesion site G* (upper panel). Efficiency $f_{ext} = (V_{max}/K_m)_{ext}$ for primer extension by a single dNTP complementary to the template base X (lower panel).

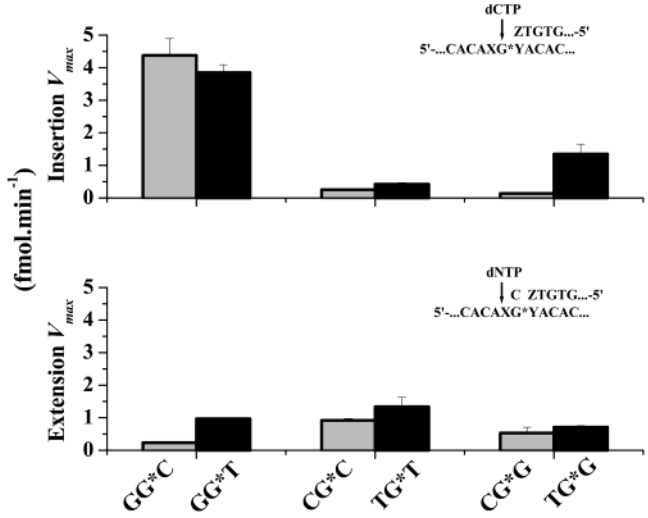

FIGURE 7: Dependence on the bases flanking the lesion G* of the steady-state value of $(V_{max})_{ins}$ (upper panel) and $(V_{max})_{ext}$ (lower panel).

region are in contact with the replicating base pair thus limiting accessibility to the aqueous environment. In Dpo4, on the other hand, the finger region is considerably smaller, and the replicating base pair is less restrained by local interactions with amino acid residues and is thus more accessible to the solvent. If the catalytic pocket in human pol κ is also relatively unconstrained, a sterically less hindered active site may facilitate interconversion between [BP]-*N*^{2}-dG adduct conformations that block bypass to conformations that are favorable for dCTP insertion opposite G*(*13*, *40*). In that case, a greater adduct conformational flexibility at the active site of pol κ may enhance the catalytic rate constant, k_{cat} (proportional to V_{max}), of dNTP incorporation opposite G*. We note that the parameter $(V_{max})_{ins}$ is not

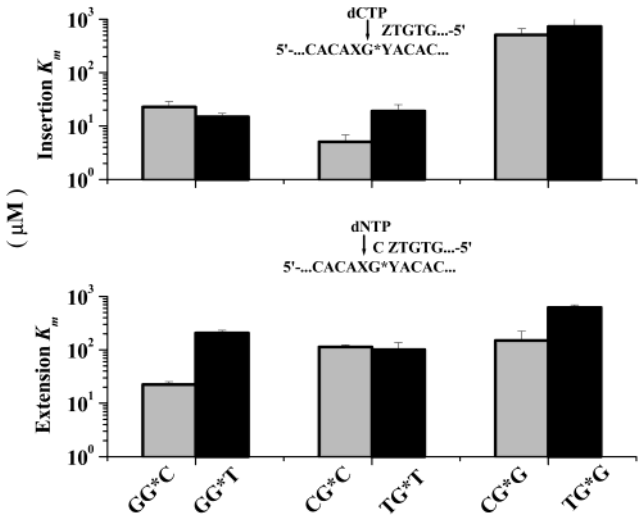

FIGURE 8: Dependence on the bases flanking the lesion G* of the steady-state value of $(K_m)_{ins}$ (upper panel) and $(K_m)_{ext}$ (lower panel).

reduced as much in the case of pol κ by the presence of (+)-*trans*-[BP]-N^2-dG adducts (Tables 1 and 2) as it is in the case of the A-family polymerase KF- (*16*). This difference may result from the lower extent of crowding in the active site of pol κ than in the active site of an A-family polymerase.

Conformations of (+)-trans-[BP]-N^2-dG Adducts in Primer/Template Complexes. The differences in the electrophoretic mobilities indicate that the flanking bases have remarkable effects on the electrophoretic mobilities, and therefore, on the adduct conformations in the (−1) but not in the (0) complexes (Figures 2 and S7). These differences are attributed to base sequence effects on the adduct conformations at the single strand−double strand junctions. The solution structures of (+)-*trans*-[BP]-N^2-dG lesions in (−1) and (0) complexes in ...CG*C... sequence contexts have been examined by NMR methods in the absence of proteins (*57*, *58*). In the (−1) complex, the hydrophobic BP residue of the (+)-*trans*-[BP]-N^2-dG lesion is stacked plane-to-plane with the 3′-terminal guanine residue of the primer strand, while the glycosidic angle of the modified guanine is in a syn rather than in the usual anti conformation (*57*). This conformation is associated with the unusually slow electrophoretic mobility in the (−1) complex with the CG*C (Figure 2), as observed in another, similar ...CG*C... sequence as well (*50*). However, in the (0) complex, the BP residue is positioned in a minor groove-like orientation pointing into the 5′-direction of the modified strand with the glycosidic angle of the modified guanine residue in the anti domain and the G*:C base pair in a Watson−Crick base pair alignment (*58*). The electrophoretic mobilities of the modified and unmodified (0) complexes are similar (Figure 2), suggesting that the lesions do not significantly perturb the overall conformations of the primer/template complexes, in contrast to the lesions in the (−1) complexes. Since the conformations of the (+)-*trans*-[BP]-N^2-dG lesions are known to depend on local base sequence context in double-stranded DNA (*42*), it is not surprising that such effects should manifest themselves at or near single-strand/double-strand junctions in solution (Figures 2 and S7) and also manifest themselves in terms of the translesion bypass kinetics. The major impact of the different bases flanking the lesions is observed when guanines are substituted for the pyrimidines. We consider some of the possible flanking base sequence effects that can account for these observations, as well as for the larger effects of sequence context on the K_m rather than on the V_{max} values.

Adverse Effects of 3′-Flanking Gs on dCTP Insertion. The large unfavorable $(K_m)_{ins}$ values, by factors of ∼50−100, observed in CG*G or TG*G sequences (relative to CG*C or TG*T sequences) (Figure 8, upper panel) are correlated with the presence of 3′-flanking Gs. Thus, a much higher dNTP concentration is required to achieve saturation of the rate of reaction in the CG*G and TG*G than in the other sequences (Figure 5). Because of the complexities and multiple steps involved in the steady-state polymerase-catalyzed primer extension, the measured apparent K_m values (Figure 5) may not be the same as either the true Michaelis−Menten parameter nor the dissociation constant K_d defining the dissociation of the dNTP from the ternary dNTP−DNA−polymerase complexes (*52*, *59*). In addition, the apparent K_m may also depend on the efficiencies of formation of the binary DNA−polymerase complexes and thus on the DNA−polymerase complex dissociation constant K_D (*60*). Therefore, alternative interpretations of the base sequence dependence of the apparent K_m values are possible. One hypothesis is that the apparent K_m values reflect a base sequence dependence of K_D. Another is that the magnitude of K_m may be related to the residence time of a dNTP (or to the relative stabilities of the catalytically productive ternary complexes) in a ternary complex in a productive conformation for nucleotide incorporation at the active site of the polymerase (*59*). Both of these properties may in turn depend on the differences in the conformations of the (−1) primer-templates as suggested by their electrophoretic mobilities (Figures 1 and S7). Detailed studies of these effects are presently under investigation in our laboratory.

The high values of K_m in the CG*G and TG*G sequences indicate that the properties of the G*G dinucleotide step are different from those of the other sequences studied. The dynamic characteristics of different dinucleotide steps are likely to be anisotropic because they depend on the repulsive and attractive interactions between the two stacked base pairs in the dinucleotide step model (*61*). These interactions govern the different structural parameters that determine the most probable relative orientations of these two base pairs. Conformational maps suggest that the energetically preferred conformations of the dinucleotide steps are quite different in the case of the 5′-GC, GT, and GG steps (*61*). The GG dinucleotide step has long been considered to be rather rigid (*62*, *63*). This rigidity may lower the local conformational flexibilities at the lesion sites, thus hindering the adoption of favorable intermediate DNA−polymerase and/or dNTP−DNA−polymerase conformations, thus giving rise to low relative efficiencies of translesion bypass in CG*G and TG*G sequences.

A second mechanism might account for the adverse effects of 3′-flanking guanines and the large enhancement of the $(K_m)_{ins}$ in CG*G as compared to CG*C sequences (*52*). Goodman et al. suggested that base-base stacking interactions of the incoming dNTP with the base at the 3′-terminus of the primer strand favor the binding of the incoming nucleotide. These base−base stacking interactions are favored when the 3′-terminal primer base is a G rather than a C

(corresponding to the CG*C or CG*G sequences, respectively).

Effects of 5′-Flanking Gs on dCTP Insertion Kinetics. The rates of dCTP incorporation and the magnitudes of $(V_{max})_{ins}$ are markedly sequence-dependent (Figures 5 and 7, respectively). The largest change in $(V_{max})_{ins}$ is observed when either the 5′-flanking C or T is replaced by a G. Thus, $(V_{max})_{ins}$ is greater by factors of ∼10 or 18 in GG*T and GG*C than in the TG*T and CG*C sequences, respectively. When the incoming dNTP is not complementary to the next template base to be replicated but is complementary to its 5′-neighboring base, the incoming nucleotide may pair with this downstream base rather than mispairing with the mismatched template base. This type of mechanism, called a dNTP-stabilized misalignment mechanism, was observed by Goodman and co-workers for primer extension catalyzed by pol *β* (*64*), by Kobayashi et al. in the case of the *DinB1* bypass polymerase pol IV (*65*), and by Kokoska et al. in the case of Dpo4 (*56*). Such sequence-dependent frameshift intermediates probably account for the −1 deletions that have been observed when pol *κ* bypasses apurinic sites (*8*). A similar mechanism appears to be operative in the case of our GG*C and GG*T sequences in which the dCTP pairs with the G flanking the modified guanine G* on the 5′-side. The dCTP can pair with G* (*I*), as well as the next downstream G by a slipped frameshift misaligned mechanism (*II*):

```
          dCTP
           ↓ZTGTG
5′-….CACAGG*YACAC…..-3′        (I)
          ↓↑
          dCTP
          ↓  ZTGTG
5′-….CACAG  YACAC…..-3′        (II)
           G*
          ↓↑
          C—ZTGTG
5′-….CACAG  YACAC…..-3′        (III)
           G*
          ↓↑
           C-ZTGTG
5′-….CACAGG*YACAC…..-3′        (IV)
```

Continuation of primer extension from (*III*) results in a −1 deletion, while full primer extension can occur if the correct alignment (*IV*) of the template/primer strands occurs after incorporation of dCTP. The differences in the length of the full extension products (Figure 3) are consistent with the sequence effect hypothesis based on mechanisms (*I*) to (*IV*). After extensive incubation times, full and prominent 43-mer primer extension bands are observed in the case of the CG*C, TG*T, TG*G, and CG*G sequences (Figure 3). However, in the case of the GG*C sequence, only a prominent 42-mer band is observed, which is consistent with the −1 deletion mechanism of primer extension from the slipped frameshift intermediate (*III*). In the case of the GG*T sequence, the most prominent band observed is also a 42-mer, but the presence of a weak 43-mer band suggests that primer extension from intermediate (*IV*) can also occur, although with a lower probability than from intermediate (*III*). The enhanced mutation efficiencies in vivo when 2-aminofluorene-dG adducts are flanked by Gs on the 5′-side (*66*) may also be due to a dNTP misalignment mechanism.

Impact of the Lesions on the Michaelis−Menten Parameters. The relatively efficient lesion bypass catalyzed by pol *κ* (Figure 3) is primarily due to the rather small impact of the (+)-*trans*-[BP]-N^2-dG lesions on the Michaelis−Menten parameter V_{max} as shown by a comparison of the V_{max} values for BPDE-modified and unmodified sequences in all sequences (Tables 1 and 2, and refs *11* and *30*)). Only the CG*G sequence is characterized by a significantly smaller value of $(V_{max})_{ins}$ (more than a factor of ∼10 smaller in the modified than in the unmodified CGG sequence). On the other hand, the K_m values are ∼2−5 orders of magnitude less favorable for both insertion and extension in the modified XG*Y sequences than in the unmodified ones, thus accounting for the small values of f_{ins} and f_{ext}.

The impact on V_{max} catalyzed by an A-family polymerase is quite different. The bypass of the same (+)-*trans*-[BP]-N^2-dG adducts has been compared in another modified and unmodified ...CGC... sequence but catalyzed by the polymerase KF- from *Escherichia coli* Pol I (*16*). The f_{ins} values were ∼5−6 orders of magnitude smaller in the BPDE-modified than in the identical unmodified sequences (*16*). In particular, the $(V_{max})_{ins}$ values were ∼100−1000 times smaller in the case of catalysis by KF-, depending on the dNTP being incorporated opposite the (+)-*trans*-[BP]-N^2-dG lesions. In contrast, in the case of the bypass of the same adducts by pol *κ*, the effects of the lesions on V_{max} are relatively small (Table 1). Translesion bypass of (+)-*trans*-[BP]-N^2-dG in the same TG*T and CG*C sequences studied here but catalyzed by KF- was reported in (*20*). Significant bypass (>5%) was observed only if slipped frameshift intermediates could occur that led to primer extension products with deletions of up to six contiguous bases. Furthermore, dATP was preferentially inserted opposite G* by KF- as in the case of T7 (Supporting Information). The effects of the large K_m values on the overall rates of translesion synthesis can be mitigated by increasing the dNTP concentrations (eq 1). The overall reaction kinetics are dictated more by V_{max} than by K_m when [dNTP] ≥ K_m, thus accounting for the relatively effective bypass of the (+)-*trans*-[BP]-N^2-dG adducts shown in Figure 3 despite the unfavorable large values of K_m. In these experiments the dNTP concentration was 100 μM, which is larger than the K_m in most of the insertion experiments, although not in the extension experiments (Figure 7). In mammalian cells, the dNTP concentrations are in the range of ∼5−20 μM (*67*), and the K_m values associated with the adducts may thus play a more determining role and thus diminish translesion bypass.

Conclusions. The kinetic parameters associated with the bypass of (+)-*trans*-[BP]-N^2-dG lesions catalyzed by pol *κ* are markedly affected by the flanking bases. The effects of more distant bases probably also play an important role and should be investigated once the effects of the flanking bases are better understood. While the effects of the adducts on catalytic rate constants, k_{cat}, associated with pol *κ* are relatively minor, the flanking bases can exert dramatically unfavorable effects on the dependence of these reaction rates on the dNTP concentrations (i.e., on the apparent K_m values). These results are interpreted in terms of the following: (1) conformational flexibilities of the BPDE-modified guanine residues in the presumably relatively open active site of the polymerase binding pockets, and (2) the probability of formation of ternary dNTP−DNA−polymerase complexes with dNTP conformations favorable for primer extension.

SUPPORTING INFORMATION AVAILABLE

Bar plots of $f_{ins} = (V_{max}/K_m)_{ins}$, $f_{ext} = (V_{max}/K_m)_{ext}$, V_{max}, K_m, and k_{cat} for the unmodified XGY sequences. Experiments depicting the fidelities of dNTP incorporation catalyzed by the replicative, A-family polymerase T7 (Sequenase version 2.0) in standing-start experiments. Experimental data depicting the gel electrophoretic mobilities of different primer/template complexes for TG*T, GG*T, and TG*G template sequences, analogous to those depicted in Figure 2. This material is available free of charge via the Internet at http://pubs.acs.org.

REFERENCES

1. Ohashi, E., Ogi, T., Kusumoto, R., Iwai, S., Masutani, C., Hanaoka, F., and Ohmori, H. (2000) *Genes Dev. 14*, 1589−1594.
2. Johnson, R. E., Prakash, S., and Prakash, L. (2000) *Proc. Natl. Acad. Sci. U.S.A. 97*, 3838−3843.
3. Gerlach, V. L., Feaver, W. J., Fischhaber, P. L., and Friedberg, E. C. (2001) *J. Biol. Chem. 276*, 92−98.
4. Ohmori, H., Friedberg, E. C., Fuchs, R. P. P., Goodman, M. F., Hanaoka, F., Hinkle, D., Kunkel, T. A., Lawrence, C. W., Livneh, Z., Nohmi, T., Prakash, L., Prakash, S., Todo, T., Walker, G. C., Wang, Z., and Woodgate, R. (2001) *Mol. Cell. 8*, 7−8.
5. Ohashi, E., Bebenek, K., Matsuda, T., Feaver, W. J., Gerlach, V. L., Friedberg, E. C., Ohmori, H., and Kunkel, T. A. (2000) *J. Biol. Chem. 275*, 39678−39684.
6. Zhang, Y., Yuan, F., Xin, H., Wu, X., Rajpal, D. K., Yang, D., and Wang, Z. (2000) *Nucleic Acids Res. 28*, 4147−4156.
7. Goodman, M. F., and Tippin, B. (2000) *Curr. Opin. Genet. Dev. 10*, 162−168.
8. Zhang, Y., Yuan, F., Wu, X., Wang, M., Rechkoblit, O., Taylor, J. S., Geacintov, N. E., and Wang, Z. (2000) *Nucleic Acids Res. 28*, 4138−4146.
9. Levine, R. L., Miller, H., Grollman, A., Ohashi, E., Ohmori, H., Masutani, C., Hanaoka, F., and Moriya, M. (2001) *J. Biol. Chem. 276*, 18717−18721.
10. Suzuki, N., Ohashi, E., Hayashi, K., Ohmori, H., Grollman, A. P., and Shibutani, S. (2001) *Biochemistry 40*, 15176−15183.
11. Zhang, Y., Wu, X., Guo, D., Rechkoblit, O., and Wang, Z. (2002) *DNA Repair 1*, 559−569.
12. Suzuki, N., Ohashi, E., Kolbanovskiy, A., Geacintov, N. E., Grollman, A. P., Ohmori, H., and Shibutani, S. (2002) *Biochemistry 41*, 6100−6106.
13. Rechkoblit, O., Zhang, Y., Guo, D., Wang, Z., Amin, S., Krzeminsky, J., Louneva, N., and Geacintov, N. E. (2002) *J. Biol. Chem. 277*, 30488−30494.
14. Harvey, R. G. (1991) *Polycyclic Aromatic Hydrocarbons: Chemistry and Carcinogenicity*, Cambridge University Press, Cambridge, UK.
15. Hruszkewycz, A. M., Canella, K. A., Peltonen, K., Kotrappa, L., and Dipple, A. (1992) *Carcinogenesis* (*London*) *13*, 2347−2352.
16. Shibutani, S., Margulis, L. A., Geacintov, N. E., and Grollman, A. P. (1993) *Biochemistry 32*, 7531−7541.
17. Hanrahan, C. J., Bacolod, M. D., Vyas, R. R., Liu, T., Geacintov, N. E., Loechler, E. L., and Basu, A. K. (1997) *Chem. Res. Toxicol. 10*, 369−377.
18. Lipinski, L. J., Ross, H. L., Zajc, B., Sayer, J. M., Jerina, D. M., and Dipple, A. (1998) *Int. J. Oncol. 13*, 269−273.
19. Alekseyev, Y. O., and Romano, L. J. (2000) *Biochemistry 39*, 10431−10438.
20. Zhuang, P., Kolbanovskiy, A., Amin, S., and Geacintov, N. E. (2001) *Biochemistry 40*, 6660−6669.
21. Mackay, W., Benasutti, M., Drouin, E., and Loechler, E. L. (1992) *Carcinogenesis (London) 13*, 1415−1425.
22. Jelinsky, S. A., Liu, T., Geacintov, N. E., and Loechler, E. L. (1995) *Biochemistry 34*, 13545−13553.
23. Moriya, M., Spiegel, S., Fernandes, A., Amin, S., Liu, T., Geacintov, N. E., and Grollman, A. (1996) *Biochemistry 35*, 16646−16651.
24. Shukla, R., Jelinsky, S., Liu, T., Geacintov, N. E., and Loechler, E. L. (1997) *Biochemistry 36*, 13263−13269.
25. Shukla, R., Liu, T., Geacintov, N. E., and Loechler, E. L. (1997) *Biochemistry 36*, 10256−10261.
26. Fernandes, A., Liu, T., Amin, S., Geacintov, N. E., Grollman, A. P., and Moriya, M. (1998) *Biochemistry 37*, 10164−10172.
27. Shukla, R., Geacintov, N. E., and Loechler, E. L. (1999) *Carcinogenesis 20*, 261−268.
28. Lenne-Samuel, N., Janel-Bintz, R., Kolbanovskiy, A., Geacintov, N. E., and Fuchs, R. P. (2000) *Mol. Microbiol. 38*, 299−307.
29. Page, J. E., Zajc, B., Oh-hara, T., Lakshman, M. K., Sayer, J. M., Jerina, D. M., and Dipple, A. (1998) *Biochemistry 37*, 9127−9137.
30. Zhang, Y., Wu, X., Rechkoblit, O., Geacintov, N. E., and Wang, Z. (2002) *Mutat. Res. 510*, 23−35.
31. Ogi, T., Shinkai, Y., Tanaka, K., and Ohmori, H. (2002) *Proc. Natl. Acad. Sci. U.S.A. 99*, 15548−15553.
32. Keohavong, P., Shukla, R., Melacrinos, A., Day, B. W., and Reha-Krantz, L. (1998) *DNA Cell. Biol. 17*, 541−549.
33. Shen, X., Sayer, J. M., Kroth, H., Ponten, I., O'Donnell, M., Woodgate, R., Jerina, D. M., and Goodman, M. F. (2002) *J. Biol. Chem. 277*, 5265−5274.
34. Chiapperino, D., Kroth, H., Kramarczuk, I. H., Sayer, J. M., Masutani, C., Hanaoka, F., Jerina, D. M., and Cheh, A. M. (2002) *J. Biol. Chem. 277*, 11765−11771.
35. Kozack, R., Seo, K. Y., Jelinsky, S. A., and Loechler, E. L. (2000) *Mutat. Res. 450*, 41−59.
36. Kozack, R. E., and Loechler, E. L. (1997) *Carcinogenesis 18*, 1585−1593.
37. Kozack, R. E., Shukla, R., and Loechler, E. L. (1999) *Carcinogenesis 20*, 95−102.
38. Kozack, R. E., and Loechler, E. L. (1999) *Carcinogenesis 20*, 85−94.
39. Seo, K. Y., Jelinsky, S. A., and Loechler, E. L. (2000) *Mutat. Res. 463*, 215−246.
40. Lee, C. H., Chandani, S., and Loechler, E. L. (2002) *Chem. Res. Toxicol. 15*, 1429−1444.
41. Fountain, M. A., and Krugh, T. R. (1995) *Biochemistry 34*, 3152−3261.
42. Geacintov, N. E., Cosman, M., Hingerty, B. E., Amin, S., Broyde, S., and Patel, D. J. (1997) *Chem. Res. Toxicol. 10*, 112−146.
43. Xu, R., Mao, B., Amin, S., and Geacintov, N. E. (1998) *Biochemistry 37*, 769−778.
44. McLaughlin, W., and Piel, N. (1984) Oligonucleotide Synthesis: a Practical Approach (Gait, M. J., Ed.) IRL Press, Oxford, UK.
45. Pirogov, N., Shafirovich, V. A., Kolbanovskiy, A., Solntsev, K., Courtney, S. A., Amin, S., and Geacintov, N. E. (1998) *Chem. Res. Toxicol. 11*, 381−388.
46. Cosman, M., Ibanez, V., Geacintov, N. E., and Harvey, R. G. (1990) *Carcinogenesis 11*, 1667−1672.
47. Geacintov, N. E., Cosman, M., Mao, B., Alfano, A., Ibanez, V., and Harvey, R. (1991) *Carcinogenesis 12*, 2099−2108.
48. Creighton, S., Bloom, L. B., and Goodman, M. F. (1995) *Methods Enzymol. 262*, 232−256.
49. Tsao, H., Rechkoblit, O., Amin, S., and Geacintov, N. E. (2000) *Polycyclic Aromatic Compounds 21*, 1−10.
50. Rechkoblit, O., Amin, S., and Geacintov, N. E. (1999) *Biochemistry 38*, 11834−11843.
51. Rechkoblit, O. Ph.D. Dissertation, New York University, New York, 2001.
52. Goodman, M. F., Creighton, S., Bloom, L. B., and Petruska, J. (1993) *Crit. Rev. Biochem. Mol. Biol. 28*, 83−126.
53. Zhou, B. L., Pata, J. D., and Steitz, T. A. (2001) *Mol. Cell. 8*, 427−437.
54. Silvian, L. F., Toth, E. A., Pham, P., Goodman, M. F., and Ellenberger, T. (2001) *Nat. Struct. Biol. 8*, 984−989.
55. Ling, H., Boudsocq, F., Woodgate, R., and Yang, W. (2001) *Cell 107*, 91−102.
56. Kokoska, R. J., Bebenek, K., Boudsocq, F., Woodgate, R., and Kunkel, T. A. (2002) *J. Biol. Chem. 277*, 19633−19638.
57. Cosman, M., Hingerty, B. E., Geacintov, N. E., Broyde, S., and Patel, D. J. (1995) *Biochemistry 34*, 15334−15350.
58. Feng, B., Groin, A., Hingerty, B. E., Geacintov, N. E., Broyde, S., and Patel, D. J. (1997) *Biochemistry 36*, 13769−13779.
59. Boosalis, M. S., Petruska, J., and Goodman, M. F. (1987) *J. Biol. Chem. 262*, 14689−14696.
60. Creighton, S., Huang, M., Cai, H., Arnheim, N., and Goodman, M. F. (1992) *J. Biol. Chem. 267*, 2633−2639.
61. Packer, M. J., Dauncey, M. P., and Hunter, C. A. (2000) *J. Mol. Biol. 295*, 71−83.
62. Hogan, M. E., and Austin, R. H. (1987) *Nature 329*, 263−266.

63. Sarai, A., Mazur, G., Nussinov, R., and Jernigan, R. L. (1989) *Biochemistry 28*, 7842−7849.
64. Efrati, E., Tocco, G., Eritja, R., Wilson, S. H., and Goodman, M. F. (1997) *J. Biol. Chem. 272*, 2559−2569.
65. Kobayashi, S., Valentine, M. R., Pham, P., O'Donnell, M., and Goodman, M. F. (2002) *J. Biol. Chem. 277*, 34198−34207.
66. Shibutani, S., Suzuki, N., Tan, X., Johnson, F., and Grollman, A. P. (2001) *Biochemistry 40*, 3717−3722.
67. Kornberg, A. (1995) *DNA Replication*, 2nd ed., W. H. Freeman and Co., New York.

BI026912Q